Quantum Phases of $SrCu_2(BO_3)_2$ from High-Pressure Thermodynamics

Jing Guo,[1] Guangyu Sun,[1,2] Bowen Zhao,[3] Ling Wang,[4,5] Wenshan Hong,[1,2] Vladimir A. Sidorov,[6] Nvsen Ma,[1] Qi Wu,[1] Shiliang Li,[1,2,7] Zi Yang Meng,[1,8,7,*] Anders W. Sandvik,[3,1,†] and Liling Sun[1,2,7,‡]

[1]*Beijing National Laboratory for Condensed Matter Physics and Institute of Physics, Chinese Academy of Sciences, Beijing 100190, China*

[2]*School of Physical Sciences, University of Chinese Academy of Sciences, Beijing 100190, China*

[3]*Department of Physics, Boston University, 590 Commonwealth Avenue, Boston, Massachusetts 02215, USA*

[4]*Beijing Computational Science Research Center, 10 East Xibeiwang Road, Beijing 100193, China*

[5]*Zhejiang Institute of Modern Physics, Zhejiang University, Hangzhou 310027, China*

[6]*Vereshchagin Institute for High Pressure Physics, Russian Academy of Sciences, 108840 Troitsk, Moscow, Russia*

[7]*Songshan Lake Materials Laboratory, Dongguan, Guangdong 523808, China*

[8]*Department of Physics and HKU-UCAS Joint Institute of Theoretical and Computational Physics, The University of Hong Kong, Pokfulam Road, Hong Kong, China*

(Received 8 September 2019; accepted 23 April 2020; published 20 May 2020)

We report heat capacity measurements of $SrCu_2(BO_3)_2$ under high pressure along with simulations of relevant quantum spin models and map out the (P, T) phase diagram of the material. We find a first-order quantum phase transition between the low-pressure quantum dimer paramagnet and a phase with signatures of a plaquette-singlet state below $T = 2$ K. At higher pressures, we observe a transition into a previously unknown antiferromagnetic state below 4 K. Our findings can be explained within the two-dimensional Shastry-Sutherland quantum spin model supplemented by weak interlayer couplings. The possibility to tune $SrCu_2(BO_3)_2$ between the plaquette-singlet and antiferromagnetic states opens opportunities for experimental tests of quantum field theories and lattice models involving fractionalized excitations, emergent symmetries, and gauge fluctuations.

DOI: 10.1103/PhysRevLett.124.206602

Theoretical proposals for exotic states in quantum magnets abound [1–6], but many intriguing quantum phases and transitions beyond classical descriptions have been difficult to realize experimentally. In one class of hypothetical states, spins entangle locally and form symmetry-breaking singlet patterns [2–10]. Signatures of a state with four-spin singlets were recently detected in the two-dimensional (2D) quantum magnet $SrCu_2(BO_3)_2$ under high pressure [11]. This plaquette singlet (PS) state has remained controversial, however [12], and a putative phase transition into an antiferromagnet (AF) at still higher pressure has not been studied. In this Letter, we report the phase diagram of $SrCu_2(BO_3)_2$ based on heat capacity measurements for a wide range of pressures P and temperatures T down to 0.4 K. Comparing the results with calculations for relevant quantum spin models, our results indicate a PS-AF transition between $P = 2.5$ and 3 GPa, which is significantly lower than previously anticipated [11].

The unpaired $S = 1/2$ Cu spins of $SrCu_2(BO_3)_2$ form layers of orthogonal dimers [13,14]. The two dominant Heisenberg exchange couplings $J_{ij}\mathbf{S}_i \cdot \mathbf{S}_j$ realize the Shastry-Sutherland (SS) model [15], illustrated in Fig. 1, with intra- and interdimer values $J' \approx 75$ K and $J \approx 45$ K, respectively. The SS model has an exact dimer-singlet (DS) ground state for $0 \leq \alpha = J/J' \lesssim 0.68$ [10,15,16] and for $\alpha \to \infty$ it reduces to the Heisenberg AF [17]. There is a PS phase between the DS and AF phases, at $\alpha \in [0.68, 0.76]$ [10,16].

At ambient pressure the properties of $SrCu_2(BO_3)_2$ agree well with the SS model in the DS phase [13,14]. AF order has been observed at $P \approx 4$ GPa [11], close to a tetragonal–monoclinic structural transition [18–20]. Since the Mermin-Wagner theorem prohibits $T > 0$ magnetic order in a 2D spin-isotropic system, the AF order should be due to weak interlayer couplings (and possibly some spin anisotropy). A 2D SS description of the quantum phase transitions is still relevant, and the simplest explanation of the behavior is that α increases with P [10,11,21]. Then it should also be possible to stabilize the PS phase of the SS model at intermediate P and low T. Breaking a discrete twofold Ising (Z_2) symmetry, corresponding to two

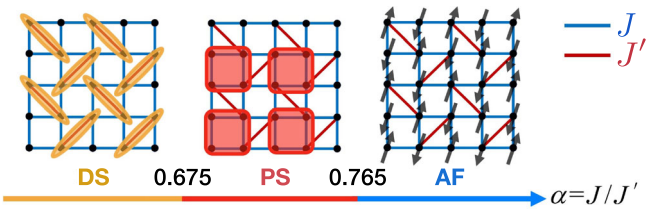

FIG. 1. Schematic $T = 0$ phase diagram of the SS model [10,16].

equivalent plaquette patterns, PS order can appear at $T > 0$ already in an isolated layer.

Following indications from nuclear magnetic resonance (NMR) of an intermediate phase with broken spatial symmetry [22,23], inelastic neutron scattering revealed an excitation attributed to a PS state [11]. The mode was only detected at $P = 2.15$ GPa, and recently an alternative scenario with no PS phase was proposed [12]. Here we argue that the PS phase exists adjacent to a previously not observed AF phase below 4 K and $P = 3$–4 GPa.

Experiments.—We have performed high-pressure heat capacity (C) measurements on $SrCu_2(BO_3)_2$ single crystals. With support of simulations of quantum spin models, we have for the first time extracted a (P, T) phase diagram, Fig. 2(a), in the range of P and T where the SS model should be relevant. Six different samples were studied, and $C(T)$ was measured from room temperature down to 1.5 or 0.4 K at several pressures (using two different types of cryostats and pressure cells; see the Supplemental Material [24]). Consistent results were obtained among all these measurements. In Figs. 2(b)–2(e) we show typical results for $C(T)/T$ in the different pressure regions. In the Supplemental Material [24] we discuss data for $P > 4$ GPa, where the SS description is no longer valid.

We identify two main low-T features in $C(T)/T$: there is always a broad maximum that we will refer to as the hump. Starting at $P \approx 1.7$ GPa, a smaller peak emerges at lower T and prevails up to 2.4 GPa. We will argue that this peak signals the PS transition. Upon further increasing P, the small peak is no longer detected at temperatures accessible in the experiments. A broader hump appears between 3 and 4 GPa, below which there is a peak at $T \approx 2$–3.5 K that we interpret as an AF transition. AF order was previously detected only at $P > 4$ GPa up to $T \approx 120$ K [11]. This high-T phase is different from the new low-T AF phase—see the Supplemental Material [24], where we also discuss a new transition at $T \approx 8$ K for $P > 4$ GPa.

The C/T hump is known from studies at ambient pressure [37], where it arises from the correlations leading to the dimer singlets as $T \to 0$. As shown in Fig. 2(a), the hump temperature $T_h(P)$, including the minimum at $P \approx 2.5$ GPa, agrees remarkably well with exact diagonalization (ED) results for the SS Hamiltonian on a 20-site lattice (see the Supplemental Material [24]) with P converted to α by linear forms $J(P)$, $J'(P)$ [11]. The hump width also agrees well with the SS model [see Fig. S5].

In the 2D Heisenberg model the hump appears at $T \approx J/2$ [38] where strong AF correlations build up. In general, the hump indicates a temperature scale where correlations set in that remove significant entropy from the system. The $T_h(P)$ minimum can be regarded as the point of highest frustration, with the energy scale being lowered due to the two competing couplings (see also Refs. [39,40]). The peak that we associate with PS ordering appears in this pressure region, suggesting singlet formation driven by strong frustration.

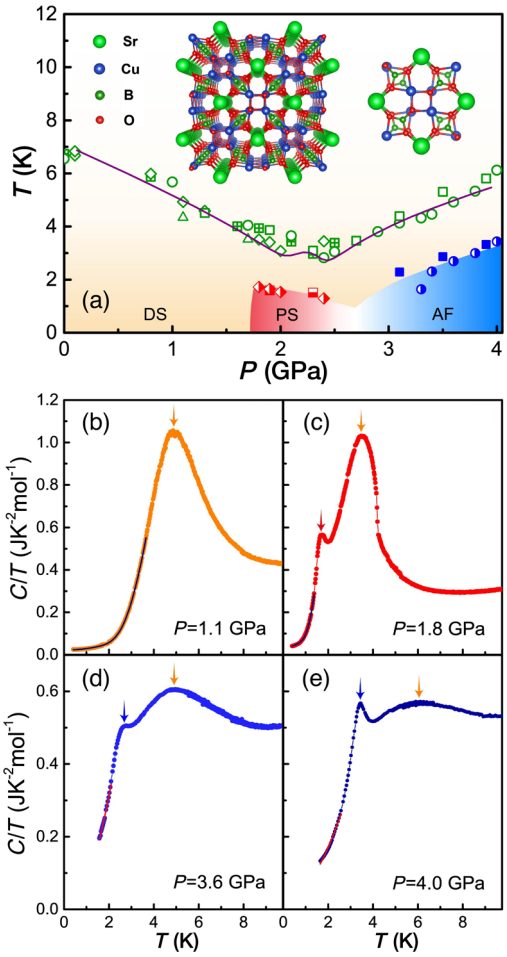

FIG. 2. (a) Phase diagram of $SrCu_2(BO_3)_2$ (crystal structure in the inset) from high pressure $C(T)$ measurements. Examples of $C(T)/T$ curves are given in (b)–(e), where the orange arrows indicate the hump location T_h. The green symbols in (a) mark T_h in several samples and the purple curve shows results for the 20-spin SS model with couplings close to those of Ref. [11]; $J'(P) = [75 - 8.3\,P/\mathrm{GPa}]\,\mathrm{K}$ and $J(P) = [46.7 - 3.7\,P/\mathrm{GPa}]\,\mathrm{K}$. For $P \approx 1.7$–2.4 GPa a second peak at lower T, marked with a red arrow in (c); it indicates the transition into the PS phase. Upon further compression, the system first enters a regime where the experiments cannot reach sufficiently low T to observe the second peak. The peak is again detectable around 3 GPa and is marked with blue arrows in (d),(e). It becomes more prominent with increasing P, suggesting [38] AF order due to weak interlayer couplings. The phase boundaries extracted from the second peak are indicated by half-filled red squares and diamonds (PS phase) and blue filled squares and half-filled circles (AF phase). The low-T data in (b),(c) are fitted (black curves) tothe form $C/T = a_0 + a_1T^2 + (a_2/T^3)e^{-\Delta/T}$ [37], giving gaps Δ shown in Fig. 3(a). In (d),(e) fits are shown (red curves) without gap term; $C/T = a_0 + a_1T^2$.

If the putative AF ordering below $T = 4$ K for $P \approx 3$–4 GPa is the result of weak inter-layer couplings $J_\perp$, the observed hump-peak separation is expected, as the hump

present for an isolated layer is not affected much by a small $J_\perp$ and $T_{AF} \to 0$ as $J_\perp \to 0$. Moreover, the ordering peak vanishes as $J_\perp \to 0$, because most of the entropy has been consumed by 2D correlations before 3D long-range order sets in. Our results at 3.6 and 4.0 GPa compare favorably with quantum Monte Carlo (QMC) calculations of weakly coupled Heisenberg layers [38] with $J_\perp/J_{2D} \approx 0.01$–$0.02$. In the SS system J_{2D} is an effective 2D AF coupling smaller than both J and J' (because of frustration). The more prominent low-T peak and higher T_{AF} at higher P should be a consequence of α increasing, likely in combination with an increase of $J_\perp$. The low-T peak becomes harder to discern as P is decreased down to 3 GPa, where T_c is lower [38]. Unfortunately, above 2.4 GPa we are restricted to $T \geq 1.5$ K and cannot track the PS and AF transitions within the white region in Fig. 2(a).

Our identification of the phases partially rely on the low-T tails in C/T. Up to $P = 2.4$ GPa we extracted the gap by fitting $C(T)/T$ to an exponential form plus terms accounting for the heater, wires, and phonons [Figs. 2(b) and 2(c)]. The P dependent gaps [Fig. 3(a)] are in excellent agreement with previous works using different methods. The gap is suddenly reduced by a factor of two at 1.7 GPa, showing that the DS-PS transition is first order, as in the SS model [10,16]. In our proposed AF phase $C(T)/T$ can be fitted [Figs. 2(d) and 2(e)] without a gap.

Figure 3(b) shows examples of the entropy obtained by integrating $C(T)/T$ in the DS, PS, and AF states. Data sets from experiments with the two different pressure cells exhibit consistent trends. Comparing the results with the SS model [Fig. 3(c)] confirms that the features in C/T below $T \approx 8$ K predominantly originate from the Cu $S = 1/2$ spin network. The agreement between the experimental and theoretical results is striking at $P = 1.3$ and 1.9 GPa, where the system is gapped. At $P = 3.9$ GPa the SS model still captures the overall magnitude of the entropy, though the AF state can naturally not be fully reproduced by a small 2D cluster.

Modeling.—Ideally, we would like to compare the experiments with the SS model supplemented by weak 3D couplings. However, calculations at low $T > 0$ in the PS and AF phases require much larger lattices than those accessible to ED, and other numerical techniques are also very challenging [39,40]. To investigate generic aspects of the PS and AF transitions, we instead study a "J-Q" model amenable to large-scale QMC simulations. The model was proposed [41] for studies of deconfined quantum criticality [2,4], and recently a "checker-board" variant (CBJQ model) was deviced for realizing the PS-AF transition [5].

The Q interactions of the CBJQ model [Fig. 4(a)] compete against AF order and lead to an unusual transition versus $g = J/Q$ where the scalar (Z_2) PS and O(3) AF order parameters combine into an O(4) vector [5]. Even though the CBJQ and SS models are different at the lattice level, one can expect universal large-scale physics. Thus,

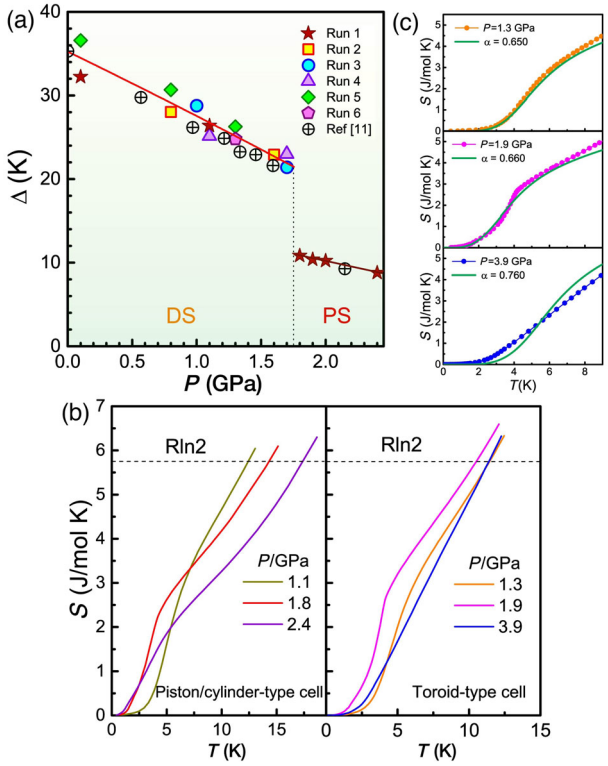

FIG. 3. (a) Pressure dependent gaps extracted from low-T fits to $C(T)/T$ [Figs. 2(b) and 2(c)] for six different experimental runs, compared with the neutron scattering results [11]; the ⊕ mark at $P = 2.15$ GPa refers to the low-energy excitation in Fig. 1 of Ref. [11]. (b) Examples of the entropy obtained by integrating C/T over T [using fits such as those in Figs. 2(b)–2(e) at low T]. (c) Results from the Toroid-type cell compared with the 20-spin SS model with couplings given by the formula used in Fig. 2(a). The results are normalized to the unit cell containing a Cu dimer; thus $S(T \to \infty) = 2R\ln(2)$ [twice the dashed line value in (b)].

$SrCu_2(BO_3)_2$ may also realize emergent O(4) symmetry—if indeed it hosts a low-T PS-AF transition dominated by 2D quantum fluctuations. Here we do not address the issue of emergent symmetry directly, but focus on the thermodynamics. The models and QMC technique are further discussed in the Supplemental Material [24].

Figure 4(b) shows C/T for different coupling ratios g in the 2D CBJQ model. The peak signaling the PS transition gradually separates from a hump as g increases, at the same time shrinking as there is less entropy associated with the phase transition. The short-range correlations signaled by the hump are predominantly AF in nature but also reflect the formation of singlets on the plaquettes before the collective ordering of those singlets. The clear hump-peak separation and the small ordering peak when $g \approx g_c$ are signatures of strong 2D quantum fluctuations of the PS order and are strikingly similar to our observations in $SrCu_2(BO_3)_2$ [Fig. 2(c)].

To study AF order at $T > 0$ we introduce interlayer couplings $J_\perp$ [Fig. 4(a)]. Figure 4(c) shows the phase

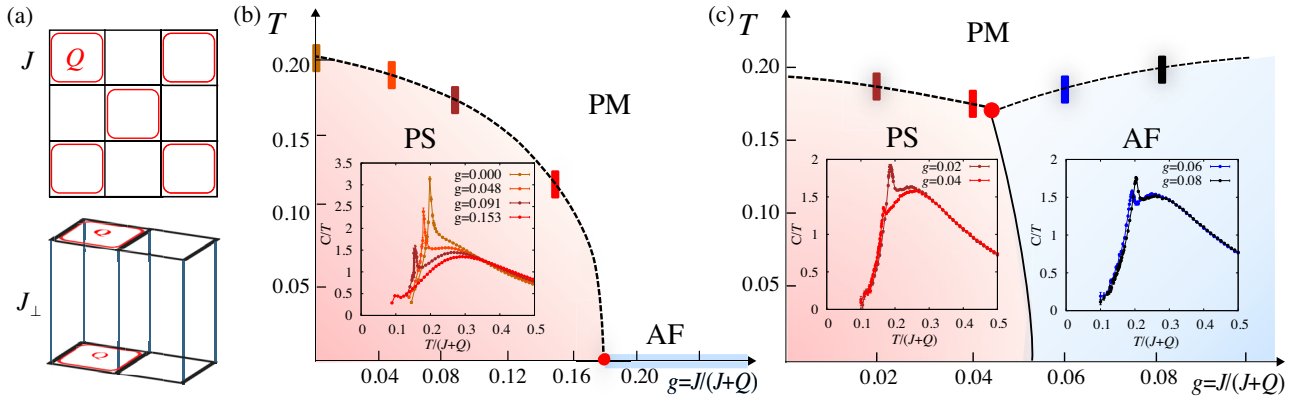

FIG. 4. (a) In the CBJQ model the SS J' exchange [Fig. 1] is replaced by four-spin interactions $-Q(\mathbf{S}_i \cdot \mathbf{S}_j - 1/4)(\mathbf{S}_k \cdot \mathbf{S}_l - 1/4)$, where ij and kl form edges (both horizontally and vertically so as to not break any symmetries) of the plaquettes with red squares [5]. Intra- and interlayer Heisenberg couplings are denoted by J and $J_\perp$, respectively. (b) $J_\perp = 0$ phase diagram with $g = J/(J+Q)$. The PS-AF quantum-critical point is at $g_c \approx 0.179$ and there is AF order only at $T = 0$. The inset shows C/T for lattices up to size 256^2 at $g < g_c$. The hump-peak separation increases and the area under the peak decreases as $g \to g_c$. (c) Phase diagram at $J_\perp/(J+Q) = 0.1$ obtained with up to $48 \times 48 \times 24$ spins. The insets show examples of $C(T)/T$ curves.

diagram for a moderately small $J_\perp$ along with scans of C/T. We observe a hump-peak structure close to the PS-AF transition; in particular the behavior in the vicinity of the AF transition is similar to the results for $SrCu_2(BO_3)_2$, thus supporting our conclusion of an AF phase in the material at $P = 3$–4 GPa.

Our SS model fit to the experimental hump in Fig. 2(a) gives $\alpha \approx 0.665$ at the DS-PS transition, close to the transition point in the SS model. In the white region in Fig. 2(a) we have $\alpha \approx 0.69$–0.71, which is smaller than $\alpha \approx 0.76$ at the PS-AF transition in the SS model. Interlayer exchange interactions will enhance the AF correlations and should shift the boundary of the AF phase in the way observed. An analogous effect of $J_\perp$ on the PS-AF transition in the CBJQ model is seen in Fig. 4 for $J_\perp = 0.1$, and even for $J_\perp = 0.01$ we still see a shift of g_c by $\approx 10\%$, as shown in the Supplemental Material [24]. We are not aware of any estimates of $J_\perp$ in $SrCu_2(BO_3)_2$, but our results show that the quantitative effects of this coupling on the phase diagram should not be neglected, even though the low-T quantum fluctuations remain predominantly 2D in nature.

Discussion.—The singlets in the PS phase of $SrCu_2(BO_3)_2$ may form on the dimer plaquettes [11], not on the empty plaquettes as in the SS model [16]. It was recently proposed that the state is not even a twofold degenerate PS state with a symmetry-breaking transition, but a state resulting from an orthorombic distortion [12]. This would be consistent with NMR results showing two kinds of dimers below 3.6 K at 2.4 GPa [23]. In our experiments, the hump in $C(T)/T$ for P between 1.7 and 2.4 GPa is close to this NMR splitting temperature, and the hump also some times has a small jump on its right side, as in Fig. 2(c). Our modeling shows clearly that the hump is a consequence of short-range correlations and does not originate from a phase transition, but the jump could still be due to a weak orthorombic transition (which might even be driven by the spin correlations). Given overall small effects on $C(T)$, such a transition (if it exists) may not change the couplings as much as suggested by Boos *et al.* [12], who also agree that the PS state can still exist with a very weak orthorombic distortion [12]. Their alternative quasi-1D state would not undergo any further phase transition at lower T, contradicting the clear peaks we find for intermediate pressures at $T \approx 2$ K. The quasi-1D scenario was in part motivated by the gap decreasing with P [as we also have found; Fig. 3(a)] [12] (see also Ref. [42] for SS model ED results). However, the gap calculations are subject to approximations, and even small interactions beyond the SS model (e.g., 3D couplings) may play a role as well in the gap evolution in $SrCu_2(BO_3)_2$. Recent ESR experiments at $P \approx 2$ GPa were explained with a PS phase surviving in the presence of a pressure-induced weak distortion [43].

In an alternative scenario, the C/T peak at $T \approx 2$ K could reflect an orthorombic transition, with the NMR splitting brought to higher T by magnetic-field effects (if the orthorombic transition is sensitive to spin correlations). However, it has also been argued from other experiments that there is no structural transition at $P \approx 2$ GPa [21,43]. It would be useful to repeat the NMR experiments for a wider range of pressures and study field effects systematically. It is also not completely clear whether the singlets in $SrCu_2(BO_3)_2$ really form on the dimer plaquettes, as calculations of the spectral signatures have only been calculated on very small systems [11] or in perturbative schemes [12] that may not sufficiently account for the complexities of the PS quantum fluctuations.

The simplest scenario is that the phase boundaries of the low-T PS and AF phases of $SrCu_2(BO_3)_2$ can be explained

by the 2D SS model with weak 3D interlayer couplings. The existence of the new low-T AF state argued here resolves a puzzling aspect of the phase diagram [11] that had not been emphasized previously: a high-T AF transition, with $T_{\mathrm{HT}} \approx 120$ K, is inconsistent with SS couplings $J, J' \ll T_{\mathrm{HT}}$ and the frustration that further reduces the effective magnetic energy scale J_{2D}. The deconfined quantum-criticality scenario for the PS-AF transition would be unlikely under these circumstances. In contrast, $T_{\mathrm{AF}} < 4$ K found here is compatible with the SS model and $J_\perp \ll J, J'$. Although we were not able to track the phase boundaries in the region $P \approx 2.4$–3.1 GPa [Fig. 2(a)], the most natural scenario is a direct PS-AF transition below $T \approx 1$ K. This transition should be weakly first order, related to the deconfined quantum-criticality scenario [2,4,44] and with an emergent O(4) symmetry of the two order parameters [5,45] if the 3D couplings are sufficiently weak. Our study has established the (P, T) region in which to further investigate this physics experimentally.

It will be important to confirm the magnetic structure of the new low-T AF phase by neutron scattering—the previous experiments in this pressure range did not reach down to the transition temperatures we found here [11]. A Raman spectroscopy study reported after the completion of our work [46] has already detected correlations compatible with AF ordering at pressures similar to Fig. 2(a). It would also be interesting to investigate magnetic field effects. Further model calculations should test the stability of the emergent O(4) symmetry [5,45] and other aspects of the PS-AF transition related to deconfined quantum criticality beyond the strict 2D limit.

The research at Chinese institutions was supported by the National Key Research and Development Program of China (Grants No. 2017YFA0302900, No. 2016YFA0300300, No. 2016YFA0300502, and No. 2017YFA0303103), the NSF of China (Grants No. 11427805, No. U1532267, No. 11604376, No. 11874401, No. 11674406, No. 11874080, No. 11421092, No. 11574359, No. 11674370 and No. 11961160699), and the Strategic Priority Research Program (B) of the Chinese Academy of Sciences (Grants No. XDB25000000, No. XDB07020000, and No. XDB28000000). The work in Boston was supported by the NSF under Grant No. DMR-1710170 and by a Simons Investigator Award. J. G. also acknowledges funding from the Youth Innovation Promotion Association of the Chinese Academy of Sciences (Grant No. 2019008) and V. A. S. acknowledges the support of RFBR Grant No. 18-02-00183. We thank the Center for Quantum Simulation Sciences in the Institute of Physics, Chinese Academy of Sciences and the Tianhe-1A platform at the National Supercomputer Center in Tianjin for their technical support and generous allocation of CPU time. Some of the numerical calculations were carried out on the Shared Computing Cluster managed by Boston University's Research Computing Services.

*zymeng@iphy.ac.cn
†sandvik@bu.edu
‡llsun@iphy.ac.cn

[1] X. G. Wen, Choreographed entanglement dances: Topological states of quantum matter, Science **363**, eaal3099 (2019).
[2] T. Senthil, A. Vishwanath, L. Balents, S. Sachdev, and M. P. A. Fisher, Deconfined quantum critical points, Science **303**, 1490 (2004).
[3] S. Sachdev, Quantum magnetism and criticality, Nat. Phys. **4**, 173 (2008).
[4] H. Shao, W. Guo, and A. W. Sandvik, Quantum criticality with two length scales, Science **352**, 213 (2016).
[5] B. Zhao, P. Weinberg, and A. W. Sandvik, Symmetry-enhanced discontinuous phase transition in a two-dimensional quantum magnet, Nat. Phys. **15**, 678 (2019).
[6] C. Wang, A. Nahum, M. A. Metlitski, C. Xu, and T. Senthil, Deconfined Quantum Critical Points: Symmetries and Dualities, Phys. Rev. X **7**, 031051 (2017).
[7] F. D. M. Haldane, O(3) Nonlinear σ Model and the Topological Distinction between Integer- and Half-Integer-Spin Antiferromagnets in Two Dimensions, Phys. Rev. Lett. **61**, 1029 (1988).
[8] N. Read and S. Sachdev, Valence-bond and spin-Peierls ground states of low-dimensional quantum antiferromagnets, Phys. Rev. Lett. **62**, 1694 (1989).
[9] L. Capriotti and S. Sorella, Spontaneous Plaquette Dimerization in the $J_1 - J_2$ Heisenberg Model, Phys. Rev. Lett. **84**, 3173 (2000).
[10] A. Koga and N. Kawakami, Quantum Phase Transitions in the Shastry-Sutherland Model for $SrCu_2(BO_3)_2$, Phys. Rev. Lett. **84**, 4461 (2000).
[11] M. Zayed *et al.*, 4-spin plaquette singlet state in the Shastry-Sutherland compound $SrCu_2(BO_3)_2$, Nat. Phys. **13**, 962 (2017).
[12] C. Boos, S. P. G. Crone, I. A. Niesen, P. Corboz, K. P. Schmidt, and F. Mila, Competition between intermediate plaquette phases in $SrCu_2(BO_3)_2$ under pressure, Phys. Rev. B **100**, 140413(R) (2019).
[13] H. Kageyama, K. Yoshimura, R. Stern, N. V. Mushnikov, K. Onizuka, M. Kato, K. Kosuge, C. P. Slichter, T. Goto, and Y. Ueda, Exact Dimer Ground State and Quantized Magnetization Plateaus in the Two-Dimensional Spin System $SrCu_2(BO_3)_2$, Phys. Rev. Lett. **82**, 3168 (1999).
[14] S. Miyahara and K. Ueda, Exact Dimer Ground State of the Two Dimensional Heisenberg Spin System $SrCu_2(BO_3)_2$, Phys. Rev. Lett. **82**, 3701 (1999).
[15] B. S. Shastry and B. Sutherland, Exact ground state of a quantum mechanical antiferromagnet, Physica (Amsterdam) **108B+C**, 1069 (1981).
[16] P. Corboz and F. Mila, Tensor network study of the Shastry-Sutherland model in zero magnetic field, Phys. Rev. B **87**, 115144 (2013).
[17] E. Manousakis, The spin-1/2 Heisenberg antiferromagnet on a square lattice and its application to the cuprous oxides, Rev. Mod. Phys. **63**, 1 (1991).
[18] I. Loa, F. X. Zhang, K. Syassen, P. Lemmens, W. Crichton, H. Kageyama, and Y. Ueda, Crystal structure and lattice dynamics of $SrCu_2(BO_3)_2$ at high pressures, Physica (Amsterdam) **359–361B**, 980 (2005).

[19] M. E. Zayed, Ch. Rüegg, E. Pomjakushina, M. Stingaciu, K. Conder, M. Hanfland, M. Merlini, and H. M. Rønnow, Temperature dependence of the pressure induced monoclinic distortion in the spin $S = 1/2$ Shastry-Sutherland compound $SrCu_2(BO_3)_2$, Solid State Commun. **186**, 13 (2014).

[20] S. Haravifard, *et al.*, Emergence of long-range order in sheets of magnetic dimers, Proc. Natl. Acad. Sci. U.S.A. **111**, 14372 (2014).

[21] S. Haravifard, A. Banerjee, J. C. Lang, G. Srajer, D. M. Silevitch, B. D. Gaulin, H. A. Dabkowska, and T. F. Rosenbaum, Continuous and discontinuous quantum phase transitions in a model two-dimensional magnet, Proc. Natl. Acad. Sci. U.S.A. **109**, 2286 (2012).

[22] S. Haravifard, D. Graf, A. E. Feiguin, C. D. Batista, J. C. Lang, D. M. Silevitch, G. Srajer, B. D. Gaulin, H. A. Dabkowska, and T. F. Rosenbaum, Crystallization of spin superlattices with pressure and field in the layered magnet $SrCu_2(BO_3)_2$, Nat. Commun. **7**, 11956 (2016).

[23] T. Waki, K. Arai, M. Takigawa, Y. Saiga, Y. Uwatoko, H. Kageyama, and Y. Ueda, A novel ordered phase in $SrCu_2(BO_3)_2$ under high pressure, J. Phys. Soc. Jpn. **76**, 073710 (2007).

[24] See the Supplemental Material at http://link.aps.org/supplemental/10.1103/PhysRevLett.124.206602 for details on the crystal growth, pressure measurements, extended phase diagram, exact diagonalization method and SS model results, and the CBJQ model, which including Refs. [25–36].

[25] H. A. Dabkowska, A. B. Dabkowski, G. M. Luke, S. R. Dunsiger, S. Haravifard, M. Cecchinel, and B. D. Gaulin, Crystal growth and magnetic behavior of pure and doped $SrCu_2(^{11}BO_3)_2$, J. Cryst. Growth **306**, 123 (2007).

[26] A. E. Petrova, V. A. Sidorov, and S. M. Stishov, High-pressure helium gas apparatus and hydrostatic toroid cell for low-temperatures applications, Physica B (Amsterdam) **359–361**, 1463 (2005).

[27] A. Eiling and J. S. Schilling, Pressure and temperature dependence of electrical resistivity of Pb and Sn from 1—300 K and 0—10 GPa—use as continuous resistive pressure monitor accurate over wide temperature range; superconductivity under pressure in Pb, Sn and In, J. Phys. F **11**, 623 (1981).

[28] A. Eichler and W. Gey, Method for the determination of the specific heat of metals at low temperatures under high pressures, Rev. Sci. Instrum. **50**, 1445 (1979).

[29] Y. Kraftmakher, Modulation calorimetry and related techniques, Phys. Rep. **356**, 1 (2002).

[30] H. Kageyama, K. Onizuka, Y. Ueda, M. Nohara, H. Suzuki, and H. Takagi, Low-temperature specific heat study of $SrCu_2(BO_3)_2$ with an exactly solvable ground state, J. Exp. Theor. Phys. **90**, 129 (2000).

[31] A. W. Sandvik, Computational studies of quantum spin systems, AIP Conf. Proc. **1297**, 135 (2010).

[32] H. J. Schulz, T. A. L. Ziman, and D. Poilblanc, Magnetic order and disorder in the frustrated quantum Heisenberg antiferromagnet in two dimensions, J. Phys. France **6**, 675 (1996).

[33] L. Wang and A. W. sandvik, Critical Level Crossings and Gapless Spin Liquid in the Square-Lattice Spin-1/2 J_1-J_2 Heisenberg Antiferromagnet, Phys. Rev. Lett. **121**, 107202 (2018).

[34] V. Yu. Irkhin and A. A. Katanin, Thermodynamics of isotropic and anisotropic layered magnets: Renormalization-group approach and $1/N$ expansion, Phys. Rev. B **57**, 379 (1998).

[35] G. Sun, N. Ma, B. Zhao, A. W. Sandvik, and Z. Y. Meng (to be published).

[36] A. Eichhorn, D. Mesterházy, and M. Scherer, Multicritical behavior in models with competing order paramaters, Phys. Rev. E **88**, 042141 (2013).

[37] H. Kageyama, H. Suzuki, M. Nohara, K. Onizuka, H. Takagi, and Y. Ueda, Specific heat study of $SrCu_2(BO_3)_2$, Physica (Amsterdam) **281&282B**, 667 (2000).

[38] P. Sengupta, A. W. Sandvik, and R. R. P. Singh, Specific heat of quasi-two-dimensional antiferromagnetic Heisenberg models with varying interplanar couplings, Phys. Rev. B **68**, 094423 (2003).

[39] P. Prelovšek and J. Kokalj, Finite-temperature properties of the extended Heisenberg model on a triangular lattice, Phys. Rev. B **98**, 035107 (2018).

[40] L. Chen, D.-W. Qu, H. Li, B.-B. Chen, S.-S. Gong, J. von Delft, A. Weichselbaum, and W. Li, Two-temperature scales in the triangular-lattice Heisenberg antiferromagnet, Phys. Rev. B **99**, 140404(R) (2019).

[41] A. W. Sandvik, Evidence for Deconfined Quantum Criticality in a Two-Dimensional Heisenberg Model with Four-Spin Interactions, Phys. Rev. Lett. **98**, 227202 (2007).

[42] H. Nakano and T. Sakai, Third boundary of the Shastry-sutherland model by numerical diagonalization, J. Phys. Soc. Jpn. **87**, 123702 (2018).

[43] T. Sakurai, Y. Hirao, K. Hijii, S. Okubo, H. Ohta, Y. Uwatoko, K. Kudo, and Y. Koike, Direct observation of the quantum phase transition of $SrCu_2(BO_3)_2$ by high-pressure and Terahertz electron spin resonance, J. Phys. Soc. Jpn. **87**, 033701 (2018).

[44] J. Y. Lee, Y.-Z. You, S. Sachdev, and A. Vishwanath, Signatures of a Deconfined Phase Transition on the Shastry-Sutherland Lattice: Applications to Quantum Critical $SrCu_2(BO_3)_2$, Phys. Rev. X **9**, 041037 (2019).

[45] P. Serna and A. Nahum, Emergence and spontaneous breaking of approximate O(4) symmetry at a weakly first-order deconfined phase transition, Phys. Rev. B **99**, 195110 (2019).

[46] S. Bettler, L. Stoppel, Z. Yan, S. Gvasaliya, and A. Zheludev, Sign switching of dimer correlations in $SrCu_2(BO_3)_2$ under hydrostatic pressure, Phys. Rev. Research **2**, 012010(R) (2020).